(12) LEVEL II

NRL Report 8469

AD A104411

High-Reliability Hydrophone Design USRD Type H68B

A. C. TIMS and C. K. BROWN

Underwater Sound Reference Detachment
P.O. Box 8337
Orlando, FL 32856

September 10, 1981

DTIC
ELECTE
SEP 21 1981
S D
B

NAVAL RESEARCH LABORATORY
Washington, D.C.

Approved for public release; distribution unlimited.

DTIC FILE COPY

81 9 21 001

NRL-8469

SECURITY CLASSIFICATION OF THIS PAGE (When Data Entered)

REPORT DOCUMENTATION PAGE	READ INSTRUCTIONS BEFORE COMPLETING FORM
1. REPORT NUMBER: NRL Report 8469 — 2. GOVT ACCESSION NO.: AD-A104411	3. RECIPIENT'S CATALOG NUMBER
4. TITLE (and Subtitle): HIGH-RELIABILITY HYDROPHONE DESIGN, USRD TYPE H68B. (9)	5. TYPE OF REPORT & PERIOD COVERED: Final report on completed work unit
	6. PERFORMING ORG. REPORT NUMBER
7. AUTHOR(s): A. C. Tims [redacted] C. K. Brown	8. CONTRACT OR GRANT NUMBER(s)
9. PERFORMING ORGANIZATION NAME AND ADDRESS: Underwater Sound Reference Detachment, Naval Research Laboratory, P.O. Box 8337, Orlando, FL 32856	10. PROGRAM ELEMENT, PROJECT, TASK AREA & WORK UNIT NUMBERS: No PE or Project, NSEA TASK 63X5-81-0019, S602-X
11. CONTROLLING OFFICE NAME AND ADDRESS: Chesapeake Naval Facility Engineering Command, Washington Navy Yard, Bldg. 57, Washington, DC 20374 (11)	12. REPORT DATE: Sep[redacted]81
	13. NUMBER OF PAGES: 39
14. MONITORING AGENCY NAME & ADDRESS (if different from Controlling Office)	15. SECURITY CLASS. (of this report): UNCLASSIFIED
	15a. DECLASSIFICATION/DOWNGRADING SCHEDULE

16. DISTRIBUTION STATEMENT (of this Report)

Approved for public release; distribution unlimited.

17. DISTRIBUTION STATEMENT (of the abstract entered in Block 20, if different from Report)

18. SUPPLEMENTARY NOTES

19. KEY WORDS (Continue on reverse side if necessary and identify by block number)

Ceramic hydrophone
Piezoelectric hydrophone
Deep-submergence hydrophones
Hydrophone design and construction
Preamplifier
High-reliability hydrophone

20. ABSTRACT (Continue on reverse side if necessary and identify by block number)

The Underwater Sound Reference Detachment of the Naval Research Laboratory has developed a state-of-the-art, deep-submergence hydrophone for use in the Underwater Tracking Range of the Atlantic Fleet Weapons Training Facility, St. Croix, that combines the best materials and craftsmanship to provide an expected service life of 20 years. The sensor provides a nominal open-circuit crystal sensitivity of −180 dB re 1 V/μPa, smooth response to frequencies above 40 kHz, omnidirectionality in the horizontal (XY) plane, and a hemispherical pattern in the vertical (XZ) plane at higher frequencies. The hydrophone has two independent preamplifiers remotely operable by a

(Continues)

DD FORM 1 JAN 73 1473 EDITION OF 1 NOV 65 IS OBSOLETE
S/N 0102-014-6601

SECURITY CLASSIFICATION OF THIS PAGE (When Data Entered)

251950

20. Abstract (Continued)

unique switching circuit. All functions — preamplifier power, signal output, and preamplifier switching — are accomplished over a coaxial cable. Established-reliability, military-specification components are used for the electronics. Specific materials used for the hydrophone and the rationale for their inclusion in the design are given.

CONTENTS

HIGH-RELIABILITY HYDROPHONE DESIGN
USRD TYPE H68B

INTRODUCTION

Tactical exercises with modern naval weapons systems should be conducted under ocean conditions, and the deep waters close to the island of St. Croix in the Virgin Islands are ideally suited for such exercises. The Underwater Tracking Range (UTR) of the Navy's Atlantic Fleet Weapons Training Facility, located in deep water off the western shore of St. Croix, uses a short-baseline tracking system for accurate three-dimensional tracking of surface and subsurface cooperative targets. The Chesapeake Division of the Naval Facilities Engineering Command (CHESNAVFAC) was tasked to expand the St. Croix UTR. A long-baseline tactical tracking range was to be established there in water up to 1400 m deep, with hydrophone cables up to 20 km long. Hydrophones with dedicated cables and support structures were to be installed to create the long-baseline acoustic-tracking capability. The remoteness and inaccessibility of the hydrophones, the cost of installation in deep water, and the demands on the tracking system dictated a need for a hydrophone design with extremely high reliability and long service life. Subsequently, CHESNAVFAC tasked the Underwater Sound Reference Detachment (USRD) of the Naval Research Laboratory to develop, design, fabricate, and evaluate a prototype of such a hydrophone.

BACKGROUND

In 1971, Groves [1] authored a report on the design of deep-submergence hydrophones. The goals and achievements in the development of a long-life, deep-submergence, wide-frequency-range hydrophone based on tried and proved designs and materials are summarized therein. It describes the USRD type H54 hydrophone, which incorporates many features that have proved successful in USRD-designed standard reference hydrophones and represents significant criteria for all deep-submergence designs.

In 1974, the Naval Torpedo Station (NTS), Keyport, Washington, asked the USRD to design a hydrophone for bottom mounting in the acoustic range at NTS. That hydrophone was to use the basic H54 housing and double boot but have a new sensor element to provide higher sensitivity, specifically desired directivity, and a preamplifier design capable of driving 8 km of coaxial cable with hydrophone power and output signal on the same cable. The hydrophone, USRD Type H68, was delivered to NTS in September 1974.

Evaluation by NTS led to the conclusion that the H68 met or exceeded design goals. Therefore, it was recommended for use in monitoring sound on the bottom of Dabob and Nanoose Ranges, and it was also recommended for use on the St. Croix range.

During FY75 and FY 76, a total of eight H68 hydrophones were constructed by the USRD for NTS. Six were sent to St. Croix, where they were mounted on short-baseline tracking arrays and installed at the UTR by CHESNAVFAC. From use of these hydrophones, it was determined that a similar or modified version would supply the requirements for a long-baseline, acoustic-tracking capability.

Manuscript submitted April 14, 1981.

SPECIFICATIONS

CHESNAVFAC advised the USRD of its desire to proceed with fabrication and testing of a prototype hydrophone either by modification of USRD Type H68 or by development of a new-design hydrophone to meet the following requirements:

- High reliability for an expected service life of 20 years.

- Military-Specification electronics.

- Redundant preamplifiers, independently powered by either a reverse power-supply polarity or reversible "latching relay" selection.

- All hydrophone functions to be performed over a dedicated coaxial cable 4 to 20 km long, terminated in its characteristic impedance.

- Capability of at least 1 V rms at the preamplifier output for maximum signal input.

- Full diode protection of the preamplifiers to prevent damage from voltage transients and acoustic overloads.

- Bandwidth from 4 to 45 kHz.

- Preamplifier gain to provide a nominal sensitivity at the preamplifier output of -140 dB re 1 V/μPa at 13 kHz when used with the H68 sensor element or a sensor of equal sensitivity.

- Depth capability of 1800 m (18 MPa).

- Hydrophone housing (all parts exposed to seawater) to be made from carbon steel, cadmium plated and a flange to be provided for mounting the hydrophone to a sea-base structure.

- Housing to accept a Morrison-seal cable-gland assembly.

HYDROPHONE GENERAL DESCRIPTION

To meet CHESNAVFAC's specified needs, the USRD developed a prototype state-of-the-art, deep-submergency hydrophone that combines the best materials and craftsmanship to provide an expected service life of 20 years. Details of the hydrophone, USRD type H68B, are shown in Fig. 1. The double butyl boots over the sensor element, with castor oil as the acoustic coupling medium, provide low permeability to water vapor and added physical protection. If the outer boot is damaged or deteriorates, the inner one can provide years of additional service. The sensor provides a nominal open-circuit crystal sensitivity of -180 dB re 1 V/μPa; smooth response to frequencies above 40 kHz; omnidirectionality in the horizontal (XY) plane; in conjunction with the baffle and a conical housing, an approximately hemispherical pattern in the vertical (XZ) plane at higher frequencies; and stability with hydrostatic pressure variations to 20 MPa. The sensor is also encapsulated in an acoustically transparent elastomer that serves as a mount, prevents fill fluid from reaching the O-rings on the end caps, and gives added protection.

The hydrophone has two independent linear preamplifiers, remotely operable by a unique switching circuit. All functions (preamplifer power, signal output, and preamplifier switching) are accomplished over a single coaxial cable. The preamplifiers are sealed in the housing, separate from the cable interface, in a nitrogen atmosphere to prevent moisture condensation with changes in temperature.

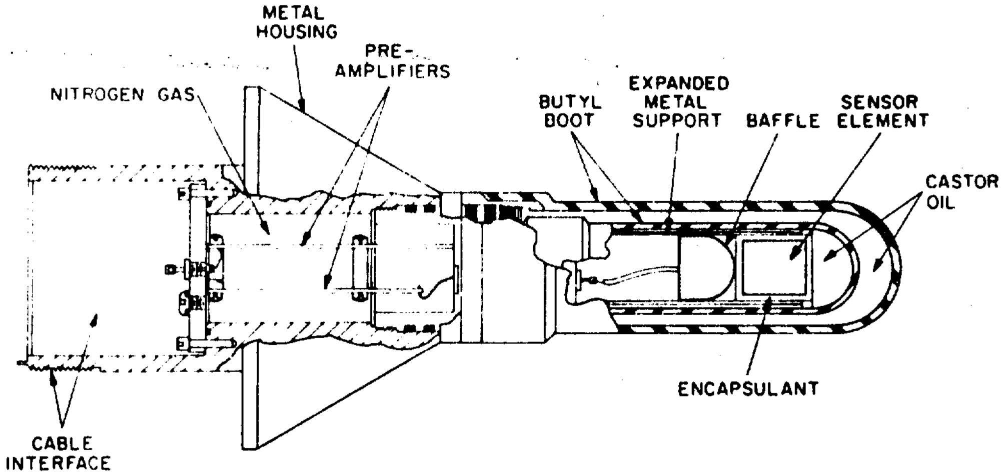

Fig. 1 — Cutaway view of USRD type H68B hydrophone

SENSITIVE-ELEMENT DESIGN

The size of the sensor element and the material from which it is made largely determine the sensitivity, directivity, and stability of the hydrophone with respect to time, temperature, and hydrostatic pressure. The constraints imposed by the bandwidth and directivity requirements place a limit on the volume of piezoelectric material that can be used in the sensor. The size of the sensor element has been selected to provide the optimum sensitivity, directivity, and electrical source impedance in a highly reliable and predictable assembly.

The acoustic sensor element is an area-ratio, unsymmetrical tonpiltz composed of a longitudinally polarized lead-zirconate-titanate cylinder with end caps and sealed by O-rings within an aluminum-oxide, precision-bore cylinder. For the sensor, shown in detail in Fig. 2, the sensitivity is simply

$$M_o = g_{33} \ell S_R \,, \tag{1}$$

where g_{33} is the piezoelectric voltage modulus for the TYPE I material (0.0245 Vm/N), ℓ is the length of the ceramic cylinder (12.7 mm), and S_R is a dimensionless quantity representing the ratio between the end-surface area of the diaphragm and the end-surface area of the crystal. If a_1 and a_2 are the inside and outside radii of the cylinder, respectively (a_1 = 5.56 mm and a_2 = 8.53 mm), and a_p is the radius of the diaphragm (11.05 mm), then

$$S_R = \frac{a_p^2}{a_2^2 - a_1^2} = 2.92 \,. \tag{2}$$

The value of M_o expressed in dB from Eq. (1) is -180.8 dB re 1 V/μPa, the open-circuit sensitivity where the sensor assembly is small compared to the acoustic wavelength. (See Appendix A, Fig. A1, for typical broad-band response.)

There are two major advantages to the length-polarized, area-ratio sensor element. First, it takes full advantage of the high sensitivity given by the g_{33} polarization vector of the ceramic by

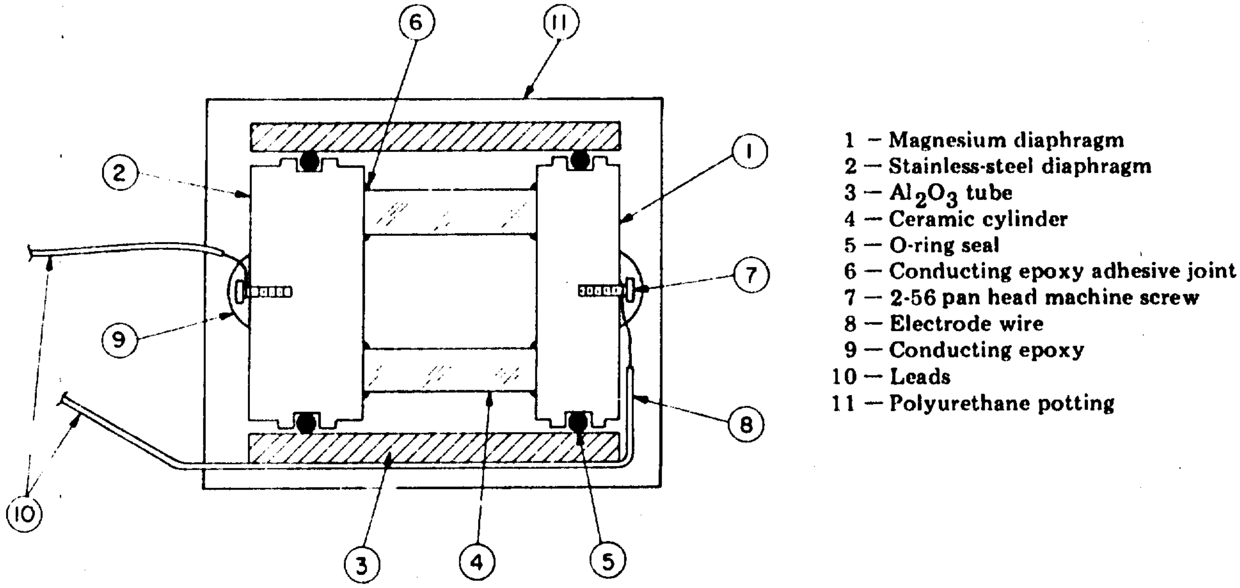

Fig. 2 — Sectional view of H68B hydrophone sensor element assembly

shielding, thus eliminating the g_{31} component. Atmospheric gases within the aluminum oxide housing and the housing itself represent an extreme impedance mismatch to the acoustic wave negating entirely the g_{31} component of the crystal. Second, the sensitivity of the crystal is effectively multiplied by the area ratio between the diaphragms and the ceramic cylinder [S_R in Eq. (1)]. The combination of these two advantages yields a high sensitivity for a small specific volume of piezoelectric material.

A major concern for the sensor assembly is its reliability. Will it last 20 years? In practice, the hydrophone is lowered to the ocean floor in water depths to about 1500 m (where the ambient temperature is about 6°C) and remains there throughout its service life. Therefore, no stress or strain is experienced by the assembly from pressure cycling or temperature excursions. The assembly is reliable enough that, in reality, the crystal could be put between the diaphragms and placed within the housing without any adhesives to bond them together. The hydrostatic pressure would compress the assembly such that a few MPa would place the diaphragms and crystal in intimate contact, and it would function just as if the assembly were bonded. Even though the assembly could be effected without adhesives, the bond between the diaphragms and the crystal is made using a high-strength conducting adhesive (conductivity of 0.0032 Ω/cm and tensile strength of 35.8 MPa). Contact of the electrode wires to the diaphragm is accomplished by tinning the electrode wire and forming a J hook and by securing the wire under the screw with conducting epoxy. A fillet of adhesive is formed around the screw and electrode wire to ensure a secure, positive electrical contact.

The housing for the tonpiltz crystal assembly is a precision-bore, 99½% pure, aluminum-oxide cylinder with an inside diameter of 22.22 mm and a nominal wall thickness of 2.0 mm. Discounting depolarization of the crystal, the assembly can safely withstand hydrostatic pressures in excess of 110 MPa. Standard O-ring practice with diametrical clearances between static and reciprocating seal tolerances, using 60-durometer nitrile O-rings, provides more than adequate sealing for the 18-MPa pressure capability.

One may ask, "What would the sensitivity of the element be if an O-ring failed and castor oil filled the sensor assembly?" Calibration of an oil-filled sensor assembly in a USRD G19 calibrator indicated a reduction of 0.3 to 0.4 dB -- not very drastic at all. The response would remain smooth until a quarter wave appeared between the two diaphragms, at about 30 kHz. However, most questions about oil invasion of the sensor assembly are moot because the entire assembly is potted in 35075 RHO-C acoustical material. The potting intimately bonds to the diaphragms and housing (an absolute requisite for any potting compound used in contact with an underwater acoustic sensor) and seals the assembly against fluid pressure; it further secures and protects the electrode-wire contact and adhesive joints.

Even though the area-ratio sensor has many advantages, it does have one major limitation. The area ratio S_R, which increases the acoustic sensitivity, also becomes a depth-limiting factor, as the stress experienced by the crystal is the hydrostatic pressure multiplied by S_R. Thus, if S_R is large the crystal experiences a one-dimensional compressive stress far in excess of the hydrostatic pressure, which must be considered in the design. Highly accurate data on the effects of one-dimensional stress on piezoelectric ceramic have been reported by Meeks, Timme, and Browder [2,3]. These references should be consulted when an area-ratio design is contemplated for use at great depths to aid in determining the best material and the stress it can stand.

DIRECTIVITY

While the sensor is inherently omnidirectional in the horizontal plane because of symmetry, it has a cardioid directivity pattern in the vertical plane with a maximum reduction in sensitivity along the $+z$ axis, but only at a single frequency. The directivity below the cardioid frequency tends to the omnidirectional with decreasing frequency; above it, with increasing frequency, the directivity tends to that of a piston until the length resonance of the assembly occurs.

When installed in the UTR, the H68B sits on top of a 4.6-m tower on the ocean floor with the z axis of the phone normal to the floor. In this manner the directivity characteristic of the sensor discriminates against bottom reflections over the frequency range of major interest.

Hugus [4] of USRD has performed the electroacoustical analysis and derived equations for the theoretical directivity of the unsymmetrical tonpiltz hydrophone sensor. That analysis is presented here in a condensed form.

When the diaphragms of the sensor are exposed to a sound field, the inner assembly vibrates about a nodal plane normal to the axial length of the piezoelectric tube. The physical parameters of the sensor configuration for this condition are shown in Fig. 3. The electroacoustic equivalent circuit, based on the assumption that the acoustic radiation and mechanical resistances are small and that it operates at frequencies below resonance, is shown in Fig. 4. The voltage/force transduction ratio is

$$\phi = (S_{33}^D \ell_c)/(d_{33} S_c) , \tag{3}$$

where S_{33}^D is the open-circuit elastic compliance in m^2/N, d_{33} is the piezoelectric constant in m/V, and S_c is the lateral end-surface area of the crystal in m^2. The mechanical compliance $C_{m1} = S_{33}^D(\ell_1/S_c)$, and $C_{m2} = S_{33}^D(\ell_2/S_c)$, in m/N. The blocked capacitance $C_e = \epsilon_b(S_c/\ell_c)$ in F, where ϵ_b = blocked permittivity in F/m.

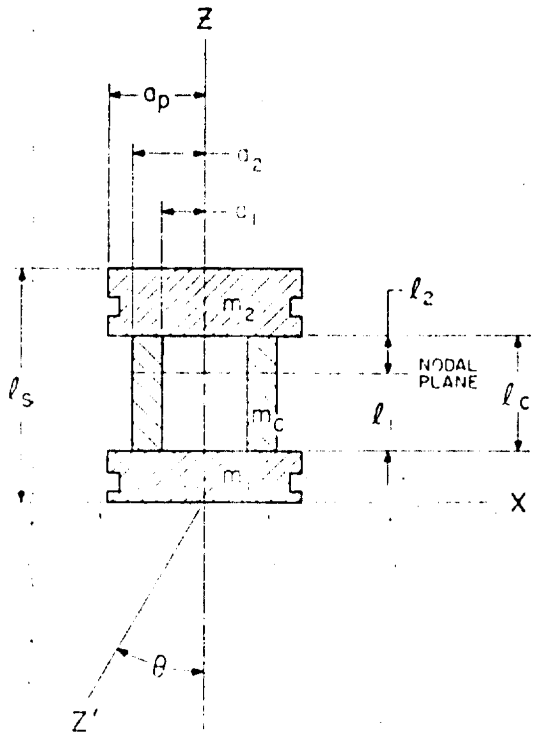

a_p — diaphragm radius (22.1 mm)
a_1 — inside radius of piezoelectric tube (5.56 mm)
a_2 — outside radius of piezoelectric tube (8.53 mm)
m_1 — mass of magnesium diaphragm (4.05 g)
m_2 — mass of stainless-steel diaphragm (22.6 g)
m_c — mass of piezoelectric tube (12.5 g)
ℓ_c — length of piezoelectric tube (12.7 mm)
ℓ_s — overall sensor length (27 mm)
ℓ_1 — distance from nodal plane to m_1
ℓ_2 — distance from nodal plane to m_2

Fig. 3 — The H68B hydrophone sensor element physical parameters

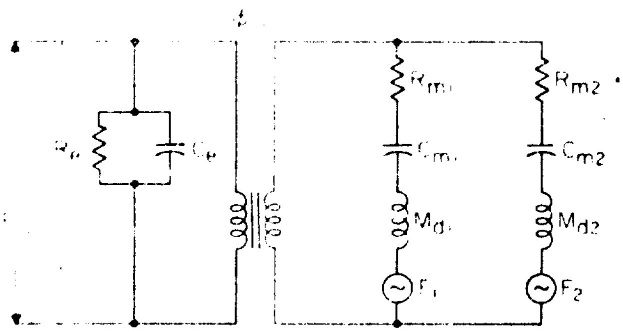

E_o is the open-circuit sensor voltage.
R_e and C_e are the blocked electrical resistance and capacitance, respectively.
ϕ is the voltage/force transduction ratio
R_{m1} and R_{m2}, C_{m1} and C_{m2} are the mechanical resistances and compliances of ℓ_1 and ℓ_2, respectively.
M_{d1} and M_{d2} are the dynamic masses on either side of the nodal plane.
F_1 and F_2 are force generators.

Fig. 4 — The H68B hydrophone sensor electroacoustic equivalent circuit

Figure 5 shows the transformed electrical equivalent circuit of Fig. 4 with the assumption that the mechanical resonances of the two mechanical branches are equal, and that

$$m_{d1} = m_1 + \left(\frac{m_c}{3}\right) \frac{(m_2 + m_c)/3}{(m_1 + m_2 + 2m_c)/3} \tag{4}$$

and

$$m_{d2} = m_2 + \left(\frac{m_c}{3}\right) \frac{(m_1 + m_c)/3}{(m_1 + m_2 + 2m_c)/3} . \tag{5}$$

Then the open-circuit voltage sensitivity of the sensor element in the vertical (XZ) plane is

$$\frac{E_o}{p} = \frac{\phi C_m S_p \left[D_m + \cos\left(k\ell_s \cos\theta\right)\right]}{(C_m + \phi^2 C_e)(D_m + 1) - \phi^2 \omega^2 C_e C_m m_{d2}} \cdot \frac{2J_1(ka_p \sin\theta)}{ka_p \sin\theta} , \tag{6}$$

where

$C_m = C_{m1} + C_{m2}$,

S_p = area of the diaphragm in m^2,

D_m is the dynamic mass ratio given by $D_m = m_{d2}/m_{d1}$,

$k = \omega/c = 2\pi/\lambda$,

c = sound velocity in m/s,

λ = wavelength in m,

$0 < \theta < 90°$, and

$J_1(ka_p \sin\theta)$ represents the first-order Bessel function of $ka_p \sin\theta$.

Equation (6) was used to generate the directivity patterns at several frequencies for comparison with actual patterns measured in the USRD Lake Facility. Figures 6 through 10 indicate the patterns,

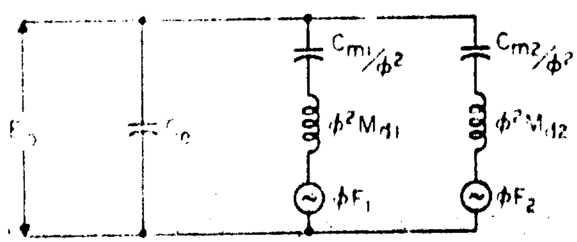

Fig. 5 — Transformed and simplified equivalent electrical circuit of Fig. 4

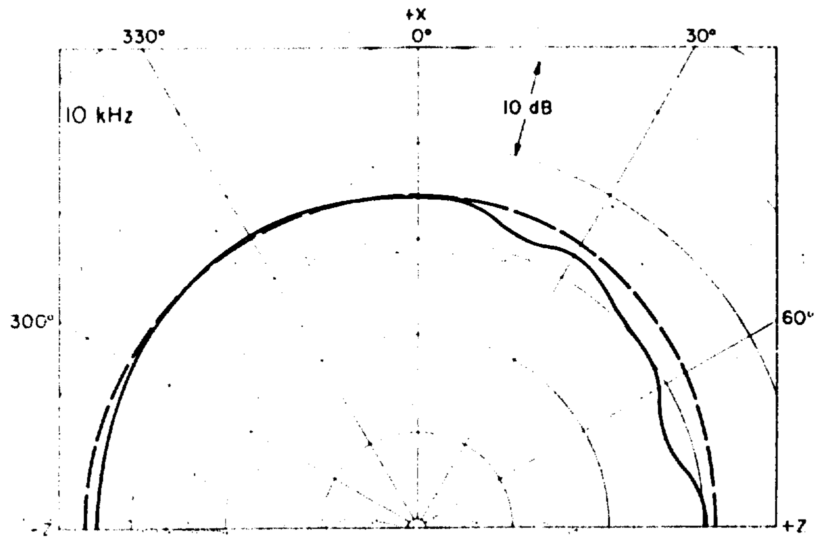

Fig. 6 — The XZ directivity pattern of the H68B hydrophone sensor element at 10 kHz, $0^\circ \leqslant \theta \leqslant 180^\circ$ (theoretical, dashed line; measured, solid line)

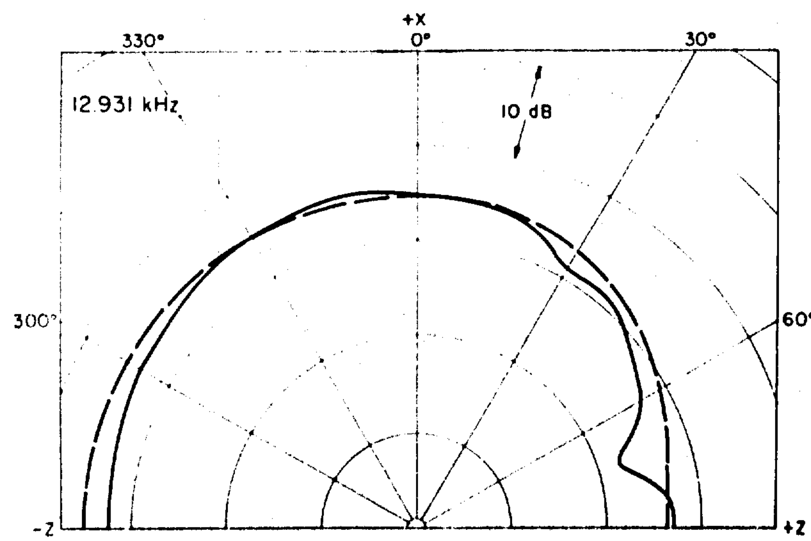

Fig. 7 — The XZ directivity pattern of the H68B hydrophone sensor element at 12.931 kHz, $0^\circ < \theta < 180^\circ$ (theoretical, dashed line; measured, solid line)

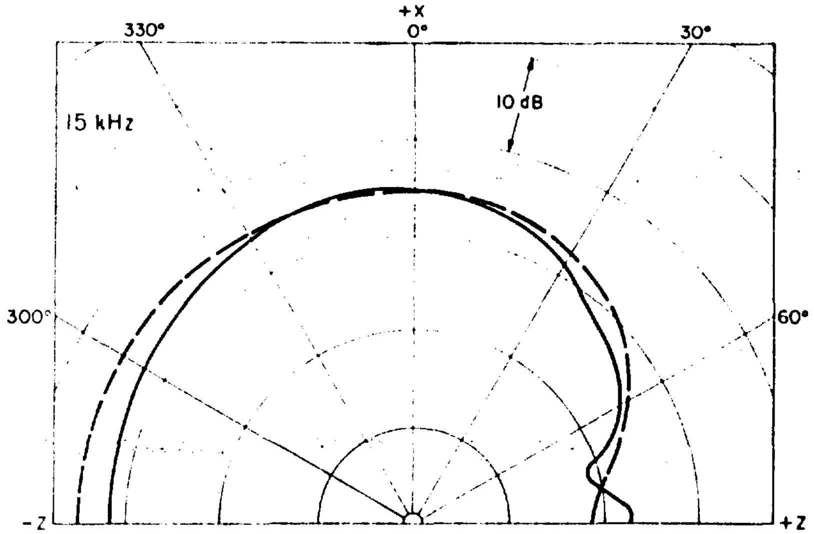

Fig. 8 — The XZ directivity pattern of the H68B hydrophone sensor element at 15 kHz, $0^\circ \leqslant \theta \leqslant 180^\circ$ (theoretical, dashed line; measured, solid line)

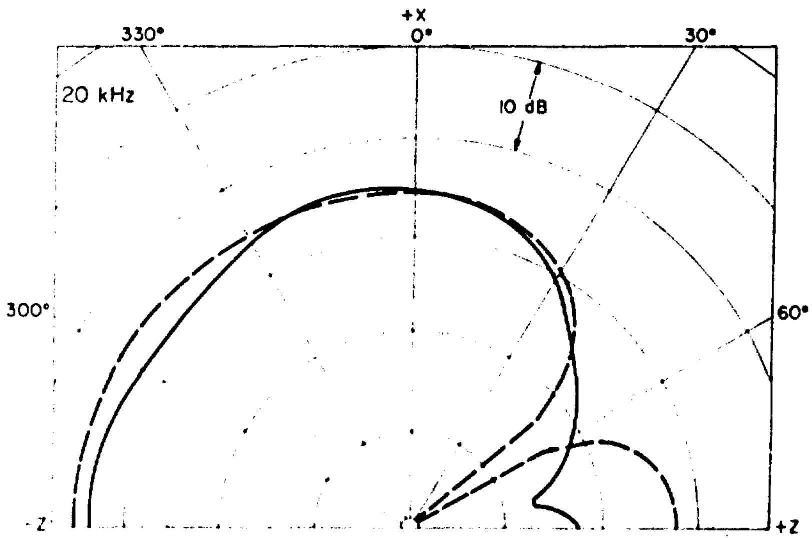

Fig. 9 — The XZ directivity pattern of the H68B hydrophone sensor element at 20 kHz, $0^\circ \leqslant \theta \leqslant 180^\circ$ (theoretical, dashed line; measured, solid line)

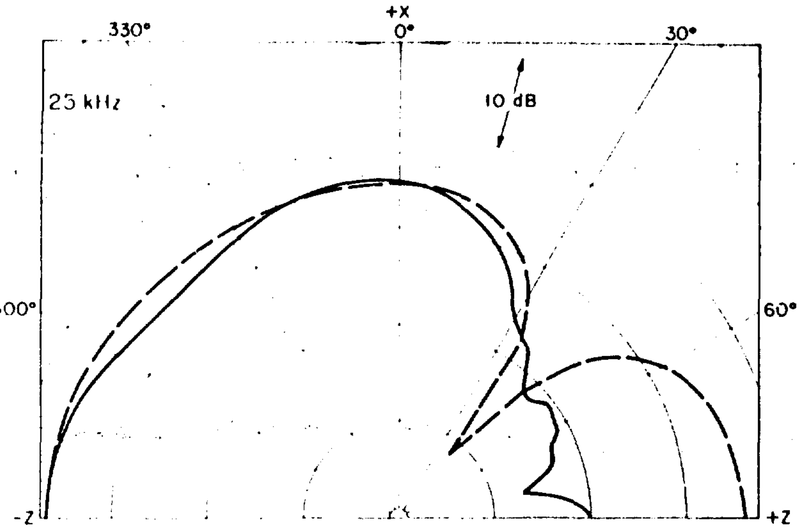

Fig. 10 The XZ directivity pattern of the H68B hydrophone sensor element at 25 kHz, $0° \leqslant \theta \leqslant 180°$ (theoretical, dashed line; measured solid line)

with the theoretical directivity indicated by the dashed plot. Only half the pattern is shown, since the other half is a mirror image of the part shown. There is good agreement between the measured and calculated plots. The worst agreement occurs at the higher frequencies. This is caused by the size of the hydrophone preamplifier housing, its proximity to the sensor assembly, and particularly by the large mounting flange.

The program sponsor wanted the large mounting flange indicated by the major diameter of the hydrophone case. The flange is necessary to secure the hydrophone to the seabed mounting structure (tower). During the early part of the hydrophone development, the flange was flat rather than conical; however, it degraded the vertical directivity of the hydrophone. The response measured on the $-z$ axis showed a series of nulls typical of standing-wave interference. In general, there are two approaches to overcoming this type of problem: move the sensor element farther away from the mounting flange, or move it as close as possible. Neither of these approaches was acceptable. Moving farther away required extending the hydrophone boots and mounting frame and was deemed too expensive because of the cost of making new boot molds. Moving closer was tried but did not yield the desired response.

The hydrophone case was redesigned to have a conical section in front of the flange. The response measured on the $-z$ axis of the hydrophone showed that the conical flange eliminated most of the reflections. Some reflections from the end of the hydrophone head were still present, but they were very small. To eliminate the remaining reflection, a machinable glass hemispherical baffle was placed close to the sensor element. The $-z$ axis response was then smooth over the frequency range of major interest. Therefore, considering the size and the proximity of the housing and the glass baffle to the sensor element, the agreement between theoretical and measured directivity patterns is quite acceptable.

MATERIALS

Design of an electroacoustic transducer for extended use in the ocean requires careful consideration of material application and compatibility with the environment. With the desired objective of high reliability and extremely long service life, it is obvious that highest quality active and passive materials should be selected. In some instances material quality is compromised because use of higher quality would make the cost of the hydrophone prohibitive. In other instances highly desirable performance characteristics may be compromised to enhance other characteristics deemed more critical. Therefore, this section will identify specific materials used for the hydrophone and the rationale for their inclusion in the design.

Active Element

Navy Type I piezoelectric ceramic [5] was chosen for the sensitive element. It has good stability with hydrostatic pressure changes for the operational depth of the hydrophone. In a one-dimensional stress configuration considering only pressure stability, Type III material would be the best choice [2,3], but the Type I material has a 30% higher dielectric constant and thus provides a lower impedance for the preamplifier. A lower source impedance results in a lower self-noise for the preamplifier [6]. The Type I material also has a slightly higher g_{33} than the Type III, which translates into about 1 dB more of sensitivity. Thus sensitivity, hydrophone self-noise, and pressure stability were the major considerations in the material choice, with the first two deemed the most important.

Aluminum Oxide

Aluminum-oxide, precision-bore tubing (Fig. 2, Item 3) was chosen to house the sensitive element. The USRD has long advocated the use of aluminum oxide, Al_2O_3, >98% pure, in sensor assemblies — especially for tonpiltz sensors and end caps for capped cylinders. The material is ideally suited for these applications because it is impervious to moisture and has high mechanical strength, a high Young's modulus, a volume resistivity $>1 T\Omega$ m ($>10^{14}$ Ω cm), and high dielectric strength. When purchased in small quantities, it not only tends to be expensive but usually has a 3- to 6-month procurement lead time. Many other materials could be substituted, such as anodized aluminum or glass tubing; but none offer the mechanical and electrical advantages of Al_2O_3.

Elastomers

The inner and outer hydrophone boots shown in Fig. 1 are made of butyl rubber. Of all the elastomers commonly used in underwater acoustics, butyl rubber has the lowest water-vapor permeability. The water permeability of most butyl compounds is 95 to 98% less than that of natural rubber, neoprene, polyurethane, Hypalon®, styrene rubbers, polyvinyl chloride, or Hycar® elastomers. Butyl rubber is easy to mold and bonds readily to metal parts properly prepared with the correct primers. The inner boot of the H68B is molded of butyl compound B252, and the outer boot of butyl compound 70821. The major difference in the two is that the latter is an electrical grade. The ingredients and physical characteristics of both of these elastomers are given by Capps [7]. The major reason for the choice of butyl is its low water-vapor permeability, because water and water vapor are responsible for most failures in underwater transducers. Butyl does not have a good ρc match to water; but if the wall section of the boot is uniform and small compared to the acoustic wavelength, it can be used successfully to frequencies beyond 100 kHz.

Fill Fluid

"DB-grade castor oil remains the most universally used liquid in transducers." The preceding statement is a direct quote from NDRC Summary Technical Report, "Design and Construction of Crystal Transducers," Volume 12 (THE RED BOOK). The irony is that 34 years after publication the statement is still true. Numerous potential fill fluids that fail to be universal in one or more properties have been investigated over the years. The salient characteristics of castor oil are high volume resistivity, close acoustic impedance match with seawater, compatibility with elastomers and other components, and stability to degradation. It is viscous and difficult to degas, but this is no problem for experienced technicians with the proper vacuum system.

The hydrophone could have been made in such a manner as to allow the head assembly to be encapsulated, thus eliminating the use of a fill fluid, but there are no general long-term immersion data available for many encapsulants. Where data are available, many have a high rate of water-vapor permeability, some are prone to bond failure, and others leach their plasticizers and become stiff or brittle. Since high reliability was the objective, the proven characteristic of a dB-grade, castor oil fluid-filled system offers much less risk than an encapsulated system. Extensive data on transducer fill fluids are found in Ref. 7.

Cable Interface

The cable interface shown in Fig. 1 accepts a Morrison cable seal. The seal, named after its designer and provided by the program sponsor, is a multilevel, coaxial, submarine cable seal that was developed at the Applied Physics Laboratory, University of Washington. It has double O-rings at the interface and is designed to seal a coaxial submarine cable (Appendix B) for 20 years at depths to 2.1 km (tested to 42 MPa and recommended for applications to 21 MPa). This seal assembly has been in service at the St. Croix UTR for several years with excellent reliability. Detailed information on the assembly is given in Ref. 8. Figure 11 shows the H68B mated with a Morrison seal.

Metal Housing

All metal parts exposed to seawater are made from AISI 1018 low-carbon steel with 0.013-mm (0.0005-in.)-thick cadmium plating, in accordance with Federal Specification QQ-P-416, Class I, Type II. The water at the St. Croix tracking range has an average oxygen content of 4 ml/l, a salinity

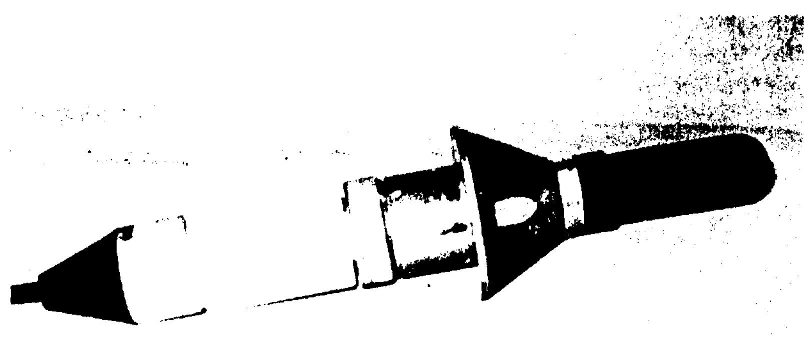

H-0102

Fig. 11 — The USRD type H68B hydrophone with Morrison Seal cable gland

of 35‰, and a temperature of 5.6°C [9]. The high oxygen content indicates a high corrosion rate; however, the waters are alkaline and the bottom sediment contains a large amount of calcium. This condition is less corrosive to steel than is normal seawater [10]. Typical corrosion rates for unplated low-carbon steel are 25 to 75 μm (1 to 3 mils) per year below 1000 m, with lower rates for longer exposures [11]. Low-carbon steels suffer from uniform corrosion and from slight crevice corrosion. The crevice corrosion can be prevented by packing all joints and O-ring grooves with silicone lubricant [12]. The suitability of using low-carbon steel in the St. Croix range environment has been proven [12], and it provides a low-cost material compatible with the concept of a 20-year service life.

ELECTRONICS

The design of an electronic system that will perform over a long time period requires considerable attention to reliability. The *Military Standardization Handbook 217B, Reliability Prediction of Electronic Equipment* was used as a guide. The handbook is oriented toward reliability prediction of military electronic equipment. It provides two methods of reliability prediction: one by parts stress analysis, and the other by parts count. Tried and proven circuits with a minimum of parts, operating under minimal electrical stress, and qualified by adherence to military specifications to the highest levels of established reliability are used in the design. The components' values, which will subsequently be given for the preamplifier circuits in the following descriptions, are identified in tabular form by value, generic description, MIL-SPEC description, and applicable military specification.

Preamplifier Requirements and Goals

Some of the requirements for the H68B preamplifier, as mentioned earlier, are:

- High-reliability design for a service life of 20 years.
- Operation over a single coaxial cable 4 to 20 km in length.
- Nominal gain of 43 dB, with bandwidth from 4 kHz to at least 45 kHz.
- Cable to be terminated in its characteristic impedance. (Cable characteristics are shown in Appendix B.)
- Maximization of dynamic range and minimization of self-noise.

These requirements tend to be incompatible, leading to design trade-offs. The final preamplifier design, described here, does meet these design goals. An alternate preamplifier approach is shown in Appendix C, and the preamplifier proof tests are described in Appendix D.

Design Approach for the Preamplifier

The preamplifier and its cable and termination are shown in simplified form in Fig. 12. To meet the requirement for high reliability, the preamplifier is redundant, consisting of identical channels A and B. However, only one channel is powered at any one time. Both dc power to the preamplifier and ac output signal from the preamplifier share the common coaxial cable. A latching relay determines which preamplifier channel is energized. The hydrophone crystal C_Y is connected to the inputs of both channels.

As shown in Fig. 12, an active termination is placed at the end of the cable. This network provides the required termination impedance for the cable. It also supplies regulated current to the preamplifier and decouples the ac and dc signal components. A MODE switch allows the user to switch from preamplifier channel A to channel B or vice versa. Should a component failure occur in one channel, the user may switch to the other channel and continue operating.

To understand the circuit operation, assume that the latching relay and MODE switch are in the positions shown in Fig. 12. Current from the $+V_{cc}$ supply is regulated to a constant value of I_{dc} in the termination network. This current flows through R_T, the cable, and R_A to zener diode CRA and preamplifier A. The diode CRA establishes a local supply voltage for preamplifier A. Preamplifier B is unenergized. Preamplifier A, therefore, amplifies the output of C_Y and couples this amplifier output signal to the cable through capacitor C_A. The signal on the cable, labeled V_A, is shown in Fig 13. It has both dc and ac components.

The dc component is blocked by capacitor C_o at the termination network, while the ac component passes through C_o to the output. Resistor R_T is made equal to the characteristic impedance of the cable. Since C_T has a very low ac impedance, the cable is effectively terminated by R_T.

The position of the latching relay is determined by the RELAY CONTROL network. This network is unenergized as long as the cable voltage is positive, which is the normal situation. In this

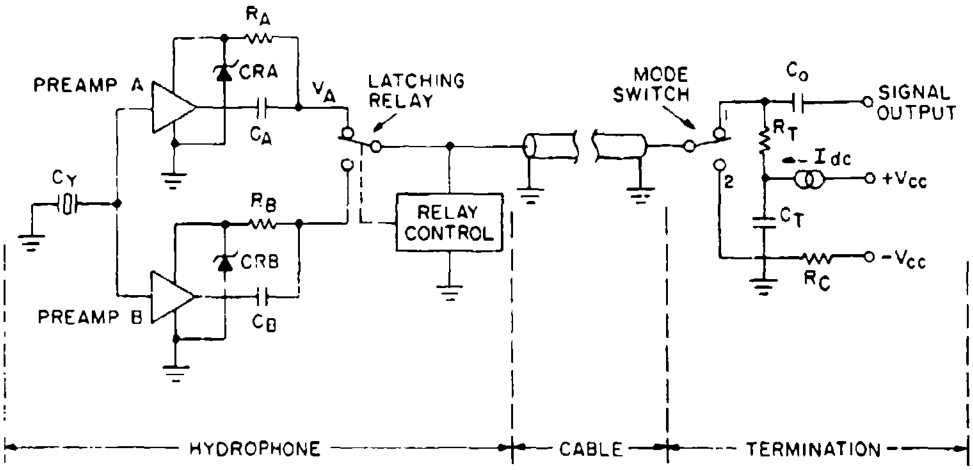

Fig. 12 — The USRD type H68B hydrophone preamplifier simplified diagram

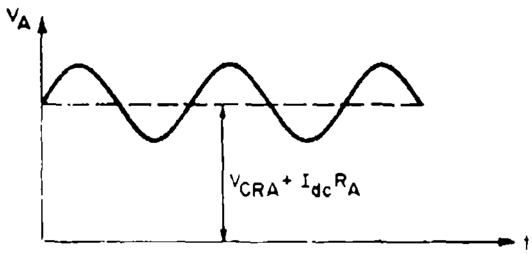

Fig. 13 — Voltage V_A on H68B hydrophone cable

case, the latching relay remains in its previously set state. To change preamplifier channels, the user activates the RELAY CONTROL network by momentarily moving the MODE switch to position 2. When this switch is returned to position 1, the RELAY CONTROL network toggles the latching relay to its alternate position. It can be seen that the MODE switch in position 2 delivers a negative dc voltage to the RELAY CONTROL network, thus activating it. The negative voltage has no effect on the preamplifier, however. Returning the MODE switch to position 1 removes the negative voltage from the RELAY CONTROL network, which causes it to toggle the latching relay.

A more detailed explanation of the RELAY CONTROL network is given later. One of the advantages of this network is that it is dc activated. It is not sensitive to rise or fall times of the cable voltage and, therefore, can be used at the end of an arbitrarily long cable. A patent has been granted for this circuit.

Detailed Description of Preamplifier

First Stage

Refer to the detailed schematic diagram in Fig. 14 (component values given in Table 1) for this description. The hydrophone crystal C_Y is to the left in this diagram. Acoustic pressures cause C_Y to produce an electric signal e_i. The amplitude of this signal is limited by diodes *CR3A*, *CR4A*, *CR3B*, and *CR4B*. As long as the signal across C_Y is less than about 0.8 V_{PK}, the diodes are essentially nonconducting and represent a very high impedance. For signals greater than this, the diodes move rapidly into their conducting region, clamping the output voltage of C_Y. This is, therefore, a safety device that protects the sensitive front end of the preamplifier from undesired voltage spikes. Such voltages could be generated, for example, by accidentally dropping the hydrophone. These are limited to about ±1 V_{PK} by the diodes, a level harmless to the preamplifier. The diodes are actually the base-collector junctions of 2N929 transistors, low-noise devices whose characteristics have been found to be ideally suited for this application.

To facilitate this discussion, only preamplifier channel A will be described. Channel B is identical. It can be seen in Fig. 14 that the signal from C_Y, e_i, is coupled through *C*1 into an FET source-follower circuit consisting of *Q*1 and *R*1 through *R*4. The load impedance that this presents to C_Y is equal to $R_i = R3 + (R1 \cdot R2)/(R1 + R2) \approx 100.1$ MΩ, since the gate of *Q*1 is back biased and therefore effectively open. The signal source is essentially capacitive and is equal to $C_i = (C_Y \cdot C1)/(C_Y + C1) \approx C_Y \approx 140$ pF, since $C1 \gg C_Y$. A high-pass filter is formed by C_i and R_i having a cutoff frequency of $1/2\pi R_i C_i \approx 11$ Hz. It can be seen, therefore, that the preamplifier front end is flat to well below the lowest frequency of interest, 4 kHz.

The gain of the source-follower circuit is approximately unity, but its output impedance is on the order of 1 kΩ. It is, therefore, an impedance transformer, which reduces the high source impedance of C_Y to about 1 kΩ.

Second Stage

The output signal at the source of *Q*1 passes directly into the second stage of the preamplifier, consisting of *A*1, *A*2, *R*5, *R*6, and *C*2. (Note that *C*6 is omitted and *R*8 is jumpered.) This is the gain stage for the preamplifier and it is also the line driver. Component *A*1 is a low-noise operational amplifier and *A*2 is a unity-gain buffer. Component *A*2 is included within the negative-feedback loop by connecting *R*6 from the output of *A*2 to the negative input terminal of *A*1. The gain of this stage is diagrammed in Fig. 15. The presence of C_2 makes the circuit gain decrease at the lower frequencies, forming a high-pass filter. The cutoff frequency is $1/2\pi \cdot R5 \cdot C2$, or about 4 kHz. Thus it is the stage that provides the required low-frequency roll-off beginning at 4 kHz. The flat

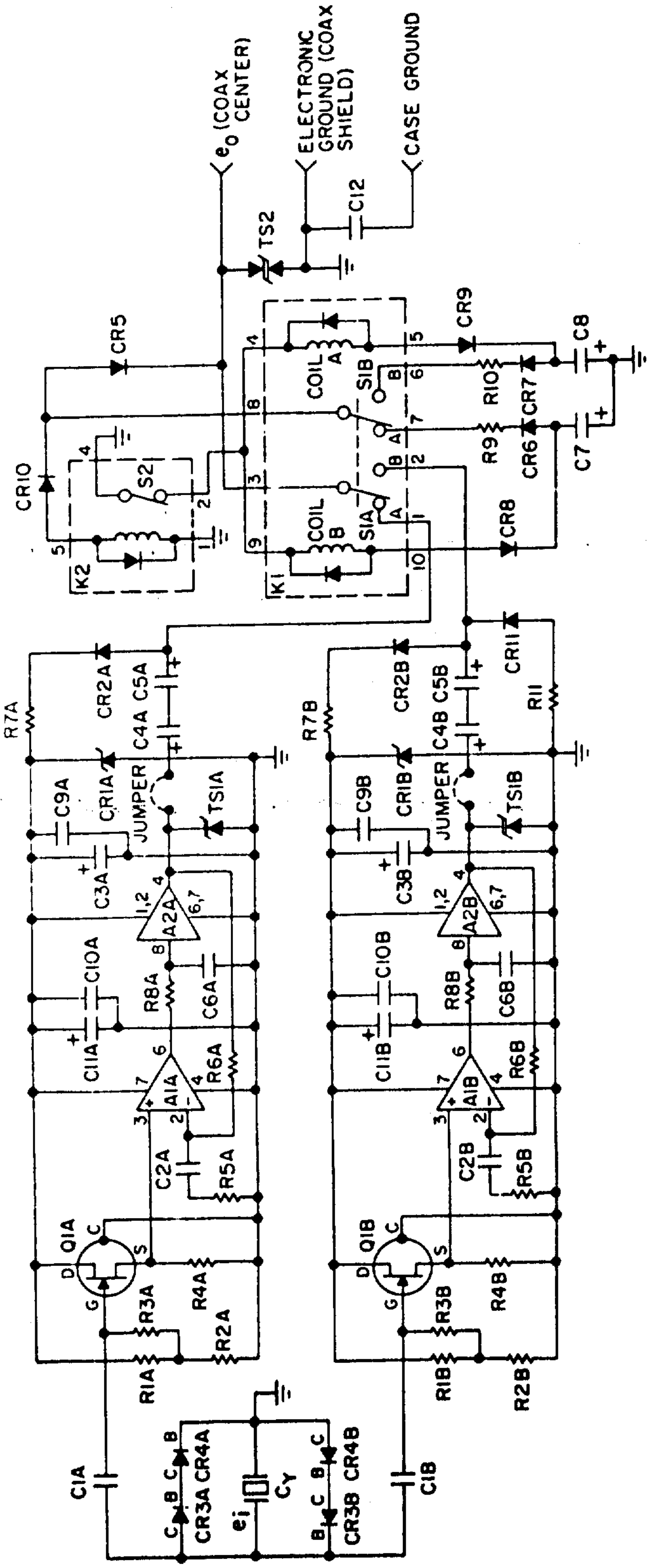

Fig. 14 — Detailed schematic of USRD type H68B preamplifier

Table 1 — Component Values for H68B (Fig. 14)

Part No.	Description	Specification	Qty. Req'd.
K2	JIMAWD-26L MIL-R-39016	HI-G	1
K1	J422D-26WL MIL-R-39016	TELEDYNE	1
TS2	IN6055A JANTXV, 40 V	G.S.I	1
TS1	IN5635A JANTXV, 10.2 V	G.S.I	2
R11	5.1 kΩ MIL-R-39008	RCR07512JS	1
R9, R10	6.8 kΩ MIL-R-39008	RCR07682JS	1 EA
R8	(JUMPER)		
R7	620 Ω MIL-R-39009B	RER40F6200R	2
R6	48.7 kΩ MIL-R-10509	RN55C4872F	2
R5	261 Ω MIL-R-55182	RNC55H2610FS	2
R4	19.1 kΩ MIL-R-55182	RNC55H1912FS	2
R3	100 MΩ ±2%	ELTEC, MODEL 104	2
R2	102 kΩ MIL-R-55182	RNC55H1023FS	2
R1	115 kΩ MIL-R-55182	RNC55H1153FS	2
C9, C10	100 pF, 200 V MIL-C-39014	CKR05BX101KS	2 EA
C7, C8	6.8 μF, 75 V MIL-C-39003	CSR13H685KR	1 EA
C6	(OMIT)		
C4, C5	15 μF, 75 V MIL-C-39003	CSR13H156KR	2 EA
C3, C11	22 μF, 35 V MIL-C-39003	CSR13F226KM	2 EA
C2	0.15 μF, 50 V MIL-C-39014	CKR06BX154KR	2
C1, C12	0.1 μF, 100 V MIL-C-39014	CKR06BX104KS	2
A2	LH0002H/883B MIL-STD-883B	NATIONAL SEMI	2
A1	SE5534A/883B MIL-STD-883B	SIGNETICS	2
CR6-CR11	1N914 JANTX MIL-S-19500		1 EA
CR3, CR4	2N929 JANTX MIL-S-19500	MOTOROLA	2 EA
CR2, CR5	IN4246 JANTX MIL-S-19500	G.S.I INC.	2
CR1	IN4744A, 15 V	G.S.I INC.	2
Q1	2N4867A	SILICONIX	2

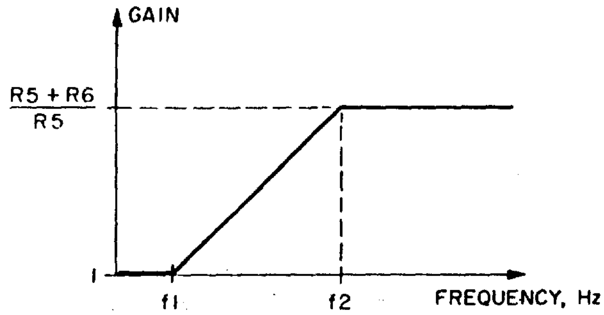

$$f1 = \frac{1}{2\pi(R5 + R6)C2} \approx 22 \text{ Hz}$$

$$f2 = \frac{1}{2\pi \cdot R5 \cdot C2} \approx 4 \text{ kHz}$$

Fig. 15 — Gain of H68B preamplifier second stage vs frequency

midband gain is given by $A = 20 \log (R5 + R6)/R5 \approx 45.5$ dB. This is made higher than the required 43 dB to compensate for a 2.5-dB loss at the front end. The source-follower gain is approximately -0.7 dB, and there is 1.8-dB coupling loss due to input capacitance loading on C_Y. Thus the overall circuit gain is 43 dB. The amplified output signal appearing at pin 4 of *A*2 is coupled through *C*4 and *C*5 and latching relay *S1A* to the coaxial cable. This cable is terminated in its characteristic impedance and presents a load of approximately 56 Ω to line driver *A*2.

Power Supply

Regulated dc power for the preamplifier is essential for proper operation. Because of the wide variation in possible cable length, 4 to 20 km, a regulated current of 31 mA dc is sent down the cable to the preamplifier. This dc current flows through *S*1*A*, *CR*2, and *R*7 to zener diode *CR*1, *A*1, *A*2, and *Q*1. This current is sufficient to supply the circuitry and cause *CR*1 to regulate at about 15 V dc. Thus *CR*1 establishes a regulated 15-V dc supply voltage for the preamplifier regardless of the cable length.

Direct-Current Biasing

Biasing for the preamplifier is established by source follower *Q*1. The source of *Q*1 is biased at approximately 7.5 V dc. This level is passed directly to the second preamplifier stage, whose gain at dc is unity. Thus the output of A_2 is also dc biased at about 7.5 V dc.

Transient Protection

Transient voltage protection is provided by components *TS*1 and *TS*2. Such transients could occur because of lightning strikes near the cable, for example, or a faulty cable termination might couple excessive voltages to the hydrophone. Component *TS*2 provides the "first line of defense" against such transients. It limits positive or negative voltages at the cable to about 45 V. The normal dc voltage at this point is positive and is equal to $V_{CR1} + I_{dc} \cdot R7 + V_{CR2} \approx 15 + (31\text{ma})(620\Omega) + 0.7 = +35$ V dc. Component *TS*2 alone would, therefore, limit positive transients to about 10 V_{PK} and negative transients to about 80 V_{PK}, but further protection is provided by *TS*1.

Consider first a negative transient. This is coupled by $C4$ and $C5$ to $TS1$, which clamps in the forward direction, protecting $A2$. This clamping action limits the amplitude of the transient to about 35 V_{PK}. The power supply is protected by the filtering action of $R7$, $C3$, and $C9$-$C11$, the clamping of $CR1$, and the back biasing of $CR2$.

In the case of a positive transient, $TS1$ breaks down at about +11.5 V. The normal output level of $A2$ is about +7.5 V. The amplitude of a positive transient is, therefore, limited to about 4 V_{PK}. The power supply would be unaffected due to the filtering action of $R7$, $C3$, and $C9$-$C11$ plus the regulation of $CR1$. Notice that $TS1$ allows a normal audio output from $A2$ of up to 4 V_{PK}, or 2.8 V_{rms}.

Relay Switching

The RELAY CONTROL network consists of components $R9$, $R10$, $C7$, $C8$, $CR5$-$CR10$, and $K2$. This network controls the state of relay $K1$ in response to a negative dc voltage applied to the cable by the user. When the cable voltage is positive (the normal situation), diode $CR5$ is back biased and the RELAY CONTROL network is idle. Since $K1$ is a latching relay, it remains in its previously programmed state until commanded to change by the control network.

Relay $K1$ contains the switch sections $S1A$ and $S1B$. It is a double-pole, double-throw (DPDT) magnetic latching relay with internal diodes, as shown in Fig. 14. Relay $K2$ is a single-pole, double-throw (SPDT) nonlatching relay in which the normally-closed (NC) contacts are used. It will operate (switch to an open condition) whenever adequate voltage is applied to its coil. In this application, relay $K2$ is rated to operate at about 26 V. However, it will actually operate at approximately 13 V and can be sustained in the open condition with only a few volts. The operation of the circuit is as follows:

(1) Assume switch sections $S1A$ and $S1B$ to be in position A as shown in Fig. 14. Also assume that the preamplifier is operating normally so that $CR5$ is back biased. Therefore $S2$ is closed and capacitors $C7$ and $C8$ are completely discharged through $S2$.

(2) Now assume that the operator wishes to switch $K1$. He removes his normal preamplifier supply voltage and applies a negative voltage ($-V$) to the cable. As $-V$ begins to rise toward its nominal value, current begins to flow through $R9$ and coil B, and $C7$ begins to charge. The value of $R9$ is chosen so that the voltage across coil B is not enough to operate $K1$. As $-V$ continues to rise, $S2$ opens. Then there is no current flow through coil B, and $C7$ charges to the full value of $-V$.

(3) To operate $K1$, $-V$ is removed. Capacitor $C7$ has no discharge path until $S2$ closes, and this only occurs when $-V$ is within several volts of ground. When $S2$ closes, $C7$ discharges through coil B and $S2$ to ground. This operates $K1$, switching $S1A$ and $S1B$ from position A to position B. Relay $K1$ is now latched in the new state.

(4) If $-V$ were reapplied by the operator, the situation would be reversed. Capacitor $C8$ would become charged. Upon removal of $-V$, $C8$ would discharge through coil A, switching $S1A$ and $S1B$ back to position A again.

The circuit operation is very much like the toggling of a flip-flop. The great advantage of the circuit is that it is dc operated. It does not depend upon the rise and fall times of $-V$, and therefore it will work with an arbitrarily long cable. United States patent number 4257082 has been granted for this circuit.

In order for the operator to determine the state of relay $K1$, components $R11$ and $CR11$ were added. When the operator tests the dc resistance of the preamplifier from the dry end of the cable, the resistance he measures will depend upon the state of $K1$. With $K1$ in position B, the shunting resistance of $R11$ and $CR11$ assures a lower resistance reading than with $K1$ in position A. Note that the polarity of the ohmmeter leads is important in this test: the positive lead must be grounded.

Grounding

The problem of grounding and stability is always important when dealing with hydrophones having preamplifiers and extremely long cables. For the H68B, zener $CR1$ establishes the "local" power supply for the preamplifier. The ground plane of the printed circuit board is true ground for the preamplifier. This is connected directly to the coaxial cable shield. A metal case surrounds the hydrophone; it makes a lossy contact to earth ground when immersed in seawater. Since earth ground is not true ground to the preamplifier, a feedback mechanism is set up in which a fraction of the preamplifier output can be returned to its input via stray capacitive coupling between the input and the metal case. This is illustrated in Fig. 16. In this figure, shield voltage e is coupled by seawater resistance R_{H_2O} to the ungrounded hydrophone case and then through C_{STRAY} to the preamplifier input, causing oscillations. To prevent this, the H68B case is connected through capacitor $C12$ to the preamplifier ground. The case is therefore ac grounded, preventing the feedback described and stabilizing the circuit.

HYDROPHONE TERMINATION

In order to test and check out the H68B hydrophones, USRD also designed a termination network, called the Hydrophone Test Set (HTS). Each HTS is housed in a small aluminum box, as pictured in Fig. 17. The HTS serves as a termination and interface to the H68B hydrophone. It provides regulated dc current to the hydrophone and decouples the audio output from the hydrophone. Using the HTS, an operator can switch preamplifier sections in the hydrophone, determine which section is operating, monitor and adjust supply current to the hydrophone, or disconnect and short the hydrophone cable.

Every effort has been made to assure that the hydrophone is protected from component failures in the HTS. A fuse mounted on the HTS printed-circuit board prevents excessive current to the hydrophone. Transient suppressors at the cable connector protect the hydrophone and the HTS from lightning-induced voltage spikes. Diodes at the HTS power-supply input terminals protect against inadvertent power-supply reversal.

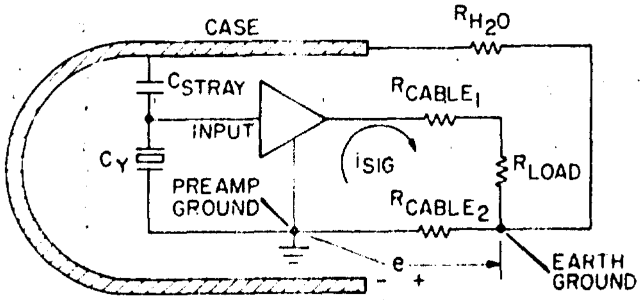

Fig. 16 — Effect of ungrounded hydrophone case

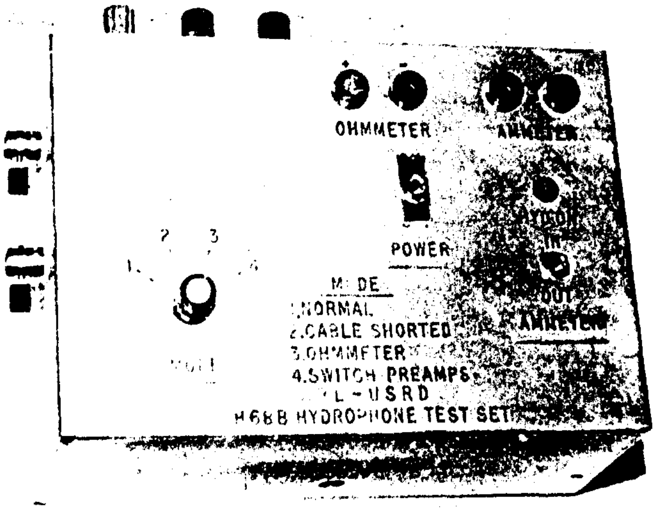

Fig. 17 — The H68B hydrophone HTS

R-0101

Theory of Operation

Refer to the HTS schematic diagram, Fig. 18 (component values shown in Table 2), for the following discussion: The HTS is powered by ±60 V dc. Normally, only the +60 V dc source is actually in use; the -60 V dc supply is used only for switching preamplifier sections in the hydrophone (to be described later). Diodes $CR1$ and $CR5$ protect the circuit from an incorrect hookup of these power supplies. Capacitors $C1$ and $C6$ provide local filtering and smoothing of the dc power; $C1$ is made large enough to prevent a sudden step of voltage from being applied to $VR1$.

Current Regulation

Because the H68B hydrophone cable can vary in length from 4 to 20 km, voltage regulation at the HTS is impractical. Instead, the hydrophone preamplifier is designed to operate on a constant supply current.

Current from the +60 V dc supply is regulated by $VR1$ to a nominal value of 31-mA dc. Regulator $VR1$ is actually a voltage-regulator device that has been externally wired to make it a current regulator. The device is "floating"; i.e., it has no ground connection. It is internally designed to maintain a nominal voltage of 1.25 V dc between the V_o and ADJ terminals. It is this feature that allows it to serve as a current regulator. If the dc output current is I_o, then $I_o = [1.25\ \mathrm{V}/(R1 + R2)\Omega]$ A, where $R1 = 30\ \Omega$ and $R2$ is 0 to 20 Ω, adjustable. By adjusting $R2$, the user sets the regulated output current to 31 mA. Since a negligibly small current (50 μA) flows into the ADJ terminal, essentially all of I_o flows through the HTS to the hydrophone. An ammeter may be connected to the AMMETER terminals on the HTS to monitor I_o. If this is done, AMMETER switch $S2$ should be opened. Otherwise, $S2$ is left closed. The HYD. ON lamp $CR4$ is illuminated when supply current is flowing to the hydrophone.

Transient suppressor $TS1$ acts as a high-speed zener to assure that the voltage from $VR1$ terminal V_i to terminal V_o can never exceed its 40-V maximum rating upon power turn-on. Components $TS1$ and $CR2$ also assure that no reverse current flows into $VR1$ upon power turn-off. Component $CR3$ prevents negative voltage transients at the ADJ terminal.

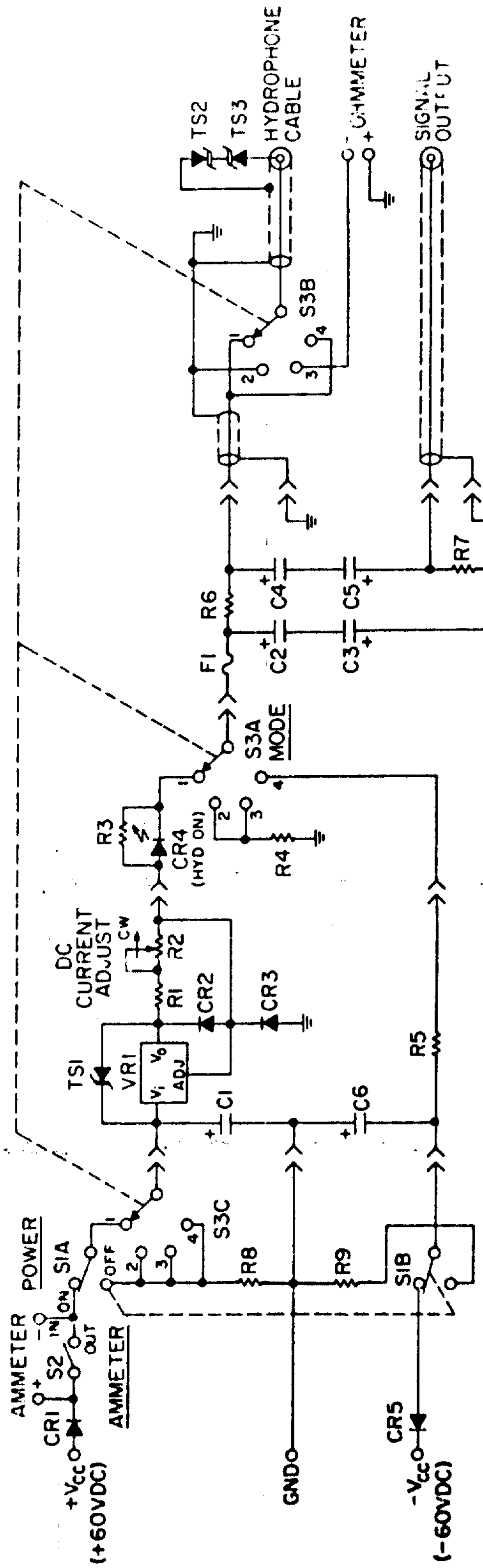

Fig. 18 — The HTS schematic diagram

Table 2 — Component Values for HTS (Fig. 18)

Part No.	Description	Specification
R7	100 kΩ ±5%, CC, 1/4 W	RCR07
R6	56 Ω ±5%, CC, 2 W	RCR42
R5	1.74 kΩ ±1%, WW, 1 W	RW-70
R4	1.5 kΩ ±5%, CC, 1/4 W	RCR07
R3	75 Ω ±5%, CC, 1/4 W	RCR07
R2	20 Ω CERMET Trimpot	IRC Type 960-20
R1	30 Ω ±5%, CC, 1/4 W	RCR07
C6	1 μF, 75 V	CSR13
C4, C5	6.8 μF, 75 V	CSR13
C2, C3	15 μF, 75 V	CSR 13
C1	400 μF, 100 V	Sprague Type TVA-1375
CR4	LED	Monsanto Type MV5021
CR1-CR3, CR5	Diode, 100 V PRV	1N4002
TS3	36 V Transient Suppressor	GSI Type 15KP36A
TS2	48 V Transient Suppressor	GSI Type 15KP48A
TS1	30.8 V Transient Suppressor	GSI Type 1N5646A
VR1	Voltage Regulator	National, LM317T
S3	3 Pole, 4 Position Switch, Nonshorting, Position 4 Momentary	Grayhill Type 83173-1-4N
S2	Switch, SPST	Alco Type TT13A-9T
S1	Switch, DPDT	C&K Type 7201
F1	Fuse, 1/20A, Subminiature	Buss Type GFA
R9	20 kΩ ±5%, CC, 1/4 W	RCR07
R8	620 kΩ ±5%, CC, 1 W	RCR 32

Test Set Modes

NORMAL Mode

Position *1* of MODE switch *S3* is the NORMAL position. When the HTS is in the NORMAL mode and the hydrophone cable is connected to the HTS, normal operation is achieved. Referring to Fig. 18, with *S3* in position *1*, the hydrophone is ON. Regulated supply current from *VR*1 flows through fuse *F*1, resistor *R*6, and switch *S3* to the hydrophone. Acoustic signals from the hydrophone are conducted directly through *C*4 and *C*5 to the SIGNAL OUTPUT connector. Resistor *R*6 provides a proper 56-Ω termination for the cable through *C*2 and *C*3 to ground. Resistor *R*7, 100 kΩ, serves as a bleeder resistor for *C*4 and *C*5.

SHORTED Mode

Position *2* of MODE switch *S3* is the CABLE SHORTED position. The hydrophone cable is shorted to ground by switch *S3*, section *B*. Section *A* of *S3* disconnects the current regulator from its load and causes *C*2 and *C*3 to discharge through *R*4. Section *C* of *S3* interrupts power to *VR*1 and allows $C1$ to discharge through $R8$. Switch $S3$ is set to position 2 whenever the hydrophone is not in use for an extended period, such as at night. This is the best position for lightning protection.

OHMMETER Mode

Position *3* of MODE switch $S3$ is the OHMMETER position. In this position, an ohmmeter connected to the HTS OHMMETER terminals will be placed directly across the hydrophone cable via switch $S3$, section B. Position *3* of $S3$ sections A and C is identical to position 2 described earlier. The hydrophone is unenergized in this position.

The HTS OHMMETER position allows the user to determine which preamplifier section is presently selected, because preamplifier section B has less dc resistance than section A. With the hydrophone at room temperature, a Fluke 8020 multimeter on the 200-kΩ scale will read about 140 kΩ if section A is selected. It will read approximately 50 kΩ if section B is selected. These readings would increase at lower temperatures. (The user must observe proper polarity when connecting an ohmmeter to the HTS.)

Resistance readings obtained in the OHMMETER position will vary from unit to unit; they are also temperature sensitive. It is not the absolute resistance readings that are important but only the relative values obtained.

SWITCHING Mode

Position *4* of MODE switch $S3$ is momentary and is used to switch preamplifier sections in the hydrophone. Each time $S3$ is switched to position *4*, a toggling action occurs in the hydrophone. For example, switching to position *4* twice could toggle the preamplifier from section A to section B and back again to A (or vice versa). Since position *4* is momentary, $S3$ returns naturally to position *3*, where an ohmmeter measurement can determine which preamplifier section is selected. The preamplifier is not energized in this position.

Preamplifier switching is achieved by placing a negative potential on the hydrophone cable of about -24 V dc. Referring to Fig. 18, when $S3$ is in position *4*, the hydrophone cable terminal is connected through $R6$, $F1$, and $R5$ to -60 V dc. Resistor $R5$ drops the -60 V level to the desired value. Capacitors $C2$ and $C3$ effectively slow the application of this potential to the hydrophone by their charging time. The exact voltage appearing at the cable connector may vary somewhat from -24 V dc, depending upon cable length and other circuit variables.

CONCLUSION

Underwater sound transducers are notorious for their poor reliability. It is not uncommon for 25% or more of the transducer elements of a sonar system to be nonfunctional after 1 or 2 years due to a variety of causes. But poor reliability need not be the case: transducers, especially hydrophones, can be built with reliability equal to space-age equipment. High reliability can be achieved through the use of reliability modeling [13], an in-depth knowledge of transducer design, careful selection of materials, and good construction techniques.

A hydrophone has been developed with an expected service life of 20 years. An array of 24 of these hydrophones has been deployed for one year. Another array of 8 hydrophones, each similar to the H68B but having only one preamplifier channel, has been deployed for four years. No failures have been reported. So, while it is still too soon to be conclusive, there is reason to believe that a 20-year-life hydrophone has been developed.

ACKNOWLEDGMENTS

The authors thank Mr. L. J. Hill of the USRD Development Section for his workmanship in assembling the hydrophones and Mr. J. Nixon of the USRD Electronics Branch for fabrication and certification of the preamplifiers.

REFERENCES

1. I. D. Groves, "The Design of Deep-Submergence Hydrophones," NRL Report 7339, Sept. 3, 1971.

2. S. W. Meeks and R. W. Timme, "Effects of One-Dimensional Stress on Piezoelectric Ceramics," J. Appl. Phys. 46, 4334-4338 (1975).

3. L. P. Browder and S. W. Meeks, "Effects of One-Dimensional Stress on MIL-STD-1376 Piezoelectric Ceramic Materials, Types I, II, and III," NRL Report 8159, Oct. 14, 1977.

4. G. D. Hugus, "Hydrophone Sensor Having a Cardioid Directivity Pattern," NRL Memorandum Report 3565, July 1977.

5. "Military Standard Piezoelectric Ceramics for Sonar Transducers," MIL-STD-1376(SHIPS) (GPO, Washington, D.C., 1970).

6. A. C. Tims, "Hydrophone Preamplifier Optimization— Prediction of Hydrophone Self-Noise by a Noise Model," NRL Report 8180, Mar. 17, 1978.

7. R. N. Capps, editor, "Handbook of Sonar Transducer Passive Materials," NRL Memorandum Report 4311, in publication.

8. "Reference Manual on Interference Seals and Connectors for Undersea Electrical Application, Naval Facilities Engineering Command," Applied Physics Laboratory, University of Washington, Seattle, Wash., July 1976 (ADA-036-841).

9. J. F. Jenkins, "Inspection of Objects Retrieved from the Deep Ocean — AUTEC Acoustic Array," Technical Note 1424, Civil Engineering Laboratory, Port Hueneme, Calif., Feb. 1976.

10. J. M. Abo, "Analysis of Array Components Recovered at St. Croix, V.I.," Report 1332, Naval Torpedo Station, Keyport, Wash., May 1977.

11. S. C. Dexter, "Handbook of Oceanographic Engineering Materials, Volume 1, Metals and Alloys," Woods Hole Oceanographic Institution, Woods Hole, Mass., Dec. 1972.

12. C. J. Sandwith, "Performance/Failure Analysis of Acoustic Array Connectors and Cables after 6-10 Years of Service," *Oceans '78*, Marine Technology Society, Washington, D.C., 1978, pp. 73-86.

13. A. C. Tims, C. K. Brown, and R. W. Timme, "Twenty-Year Life Hydrophones," presented at Institute of Acoustics Conference, Birmingham, England, Dec. 16, 1980.

Appendix A

CONSTRUCTION TECHNIQUES FOR H68B SENSOR ASSEMBLY

The area ratio sensor assembly with metal diaphragms and an aluminum oxide housing has been used by the USRD in several standard hydrophones for many years. Experience has shown the sensor assembly to be reliable, to be easy to construct, and to have a predictable response. However, some difficulty was experienced when the element was encapsulated. What was usually a straightforward and simple assembly became quite complicated and had a very unpredictable response. Obviously the problem was related to the potting or the potting procedures. Investigation of the problem showed the potting procedure to be a part of the problem but not all of it.

The response of the encapsulated sensor element was uncharacteristic at low hydrostatic pressures at frequencies between 10 and 40 kHz, but at high pressure the response was normal. It was found that the small interstices between the diaphragms and the sensor housing are nearly impossible to fill completely. The small diametrical clearances required for the O-rings at high pressures with a highly viscous potting compound amplify the problem. Since the diaphragm is relatively thick on the H68B sensor, the depth of the interstice is also a factor making the small void even more difficult to fill. A gas bubble trapped down in the slit near the O-ring groove is impossible to detect visually. Since the bubble is enclosed by rigid boundaries, it resonates at much higher frequencies than those normally encountered for gas bubbles.

Since primers were used to enhance the bond between the elastomer and the sensor element, it was suspected that the primer was sealing the diaphragm slit or going down into the slit and forming a rigid coupling. A sealed slit could certainly cause improper filling and result in the response characteristic just described. Acoustic tests and physical examination of the sensor element also showed that the priming could result in a locked diaphragm. A diaphragm rigidly coupled to the housing (locked) appears acoustically as a sharp glitch at mid-frequencies and as an oblate directivity pattern in the horizontal plane. Since the 35075 acoustical material used to pot the element bonds tenaciously to most materials without primers, and since the hydrostatic pressure at operational depth would maintain bond intimacy, the primer was eliminated from the potting procedure. Elimination of the primer resulted in a partial solution; it was still impossible to fill the slit completely more than 40 to 50% of the time.

The ultimate solution was achieved when the diaphragms were undercut as shown in Fig. 2 (main text) to allow more space. Care still must be exercised in the potting procedure for 95 to 100% confidence of success. First one and then the other diaphragm slit must be vacuum filled prior to potting of the entire assembly. If this is done first, then the chances for success are very high.

It should be noted that USRD transducer personnel are not novices in the area of potted transducer assemblies; some have more than 20 years of experience in potting and encapsulating. This emphasizes that care and experience are necessary to successfully encapsulate such a sensor assembly.

Another important point in the assembly is that the diaphragms must not rub or bind in the housing. They must be centered by O-rings during assembly of the transducer element. The inside surface of the housing and the O-rings should be well lubricated with silicone grease, BUT this should be done judiciously to prevent silicone contamination of any surface to be bonded.

Figure A1 shows a typical H68B response curve along with curves for sensor assemblies with air trapped in the diaphragm slit and for a sensor with a locked diaphragm or a diaphragm that is rubbing on one side of the transducer housing.

The following is a summary of critical points for the encapsulation of an area ratio type sensor element:

(1) Undercut diaphragms to enlarge the interstices between diaphragms and housing.

(2) Inspect diaphragms for sharp edges, burrs, and adherence to dimensional tolerances.

(3) Assemble and bond crystal element and diaphragms in the precision bore housing with O-rings grooved to ensure proper centering. The O-rings should be notched to allow gases to escape as the adhesive cures.

(4) Remove notched O-rings from assembly and clean all parts prior to potting.

(5) Judiciously lubricate ends of housing and O-rings. Groove one O-ring on a diaphragm and carefully slip assembly into housing, ungrooved diaphragm first. Continue pushing in until O-ring seats and assembly protrudes just beyond the housing to allow grooving of the other O-ring. Groove other O-ring and push assembly back into housing into proper position. Make sure the diaphragms are free to move and do not bind or touch the housing.

(6) Pot each diaphragm-housing slit with diaphragm in vertical position prior to encapsulating the assembly.

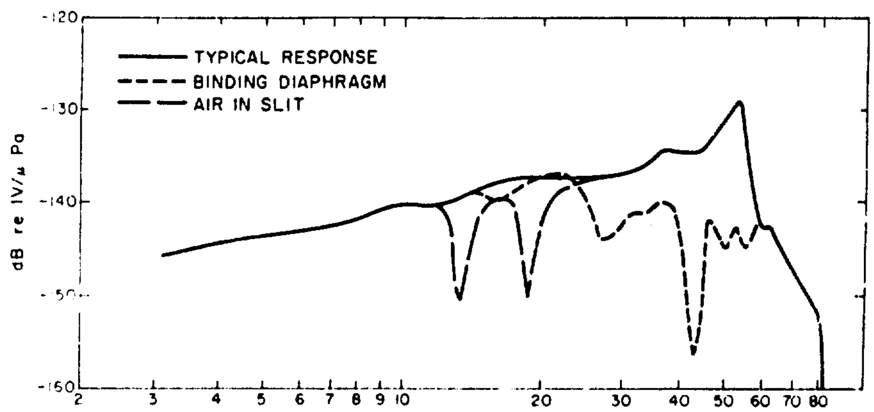

Fig. A1 — Response curves for H68B at output of preamplifier for various sensor conditions

Appendix B

CABLE SPECIFICATIONS FOR H68B HYDROPHONE

The following specification is from the Simplex Wire and Cable Co., Hydrospace Systems Division, for the 0.057-in./0.180-in. (1.45-mm/4.57-mm) Caged Armor Coaxial Cable used on the H68B hydrophone. The cable is intended for use as a communcation circuit for underseas operations. It is made up of the following components:

Central Conductor: One 1.45-mm (0.057-in.)-diameter, solid, soft-copper conductor of high quality and purity, not tinned.

Insulation: High-quality and high-purity polyethylene extruded to a diameter of 4.57 mm (0.180 in.).

Return Circuit: Three 0.41-mm (0.016-in.)-thick X 4.98-mm(0.196-in.)-wide, uncoated, soft-copper tapes of high quality and high purity, spirally applied. The diameter over the tape is approximately 5.3 mm (0.21 in.).

Shielding: One 0.076-mm (0.003-in.)-thick X 19.0-mm (0.75-in.)-wide, uncoated, soft-copper tape of high quality and high purity, applied with overlap. Diameter over the tape is approximately 5.6 mm (0.22 in.).

Belt: High-quality and high purity polyethylene extruded to a 9.65-mm (0.380-in.) diameter.

Caged Armor Wires for Deep-Sea Cable: Twelve 1.09-mm (0.043-in.)-diameter, extra-high-strength, galvanized-steel armor wires, evenly spaced around the cable.

Outer Jacket: Black high-density polyethylene applied concurrently with the armoring operation to surround and cover the armor wires completely to a diameter of approximately 16.8 mm (0.66 in.). Near the shore the cable transitions from a deep-sea configuration to a shore-cable configuration.

Armor for Shore Cable: Twenty-five 2.18-mm (0.086-in.)-diameter, galvanized, extra high-strength steel wires applied over deep-sea cable. Each wire is coated with preservative tar compound. The diameter over the armor wires is approximately 21 mm (0.83 in.).

Outer Covering: Two servings of 17/3 jute-nylon yarn with a flooding of tar preservative compound between and over each serve. The overall diameter is approximately 27.2 mm (1.07 in.).

CALCULATED CABLE DATA

Deep-Sea Type

Overall Diameter	**16.8mm (0.66 in.)**
Weight in Air	**362 kg/km (1,480 lb/nmi)**
Weight in Seawater	**164 kg/km (550 lb/nmi)**
Minimum Breaking Strength	**1800 kg (4,000 lb)**

Armored Shore Type

Overall Diameter	27.2mm (1.07 in.)
Weight in Air	1266 kg/km (5,170 lbs/nmi)
Weight in Seawater	825 kg/km (3,370 lb/nmi)
Minimum Breaking Strength (Caged Armor Only)	1800 kg (4,000 lb)

loop resistance = 13.8 Ω/km (4.2 Ω/1000 ft)
capacitance = 0.109 μF/km (0.202 μF/nmi)

The attenuation and the characteristic impedance as a function of frequency are shown in Fig. B1.

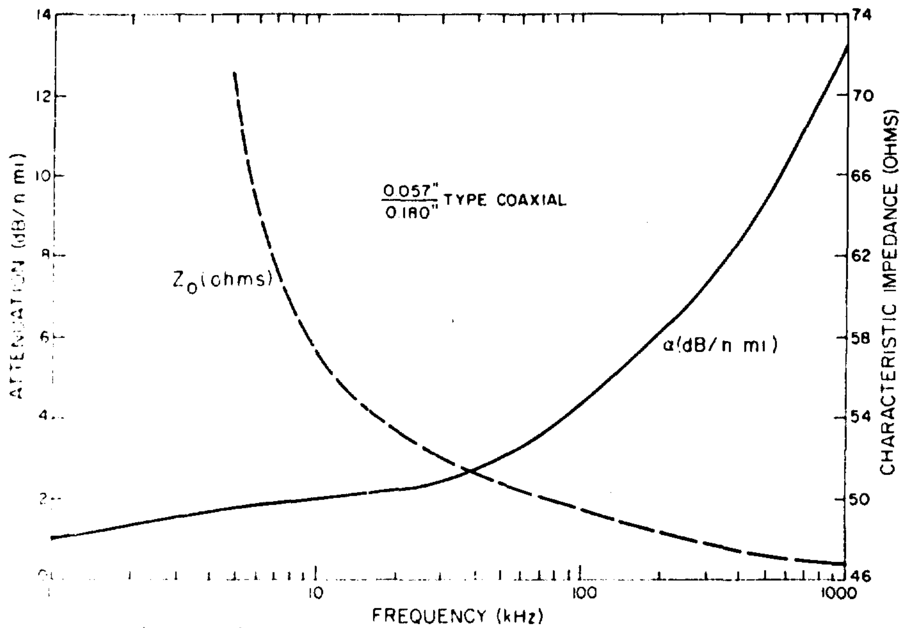

Fig. B1 — Attenuation and characteristic impedance of cable as a function of frequency

Appendix C

AN ALTERNATE PREAMPLIFIER APPROACH

This appendix describes briefly an alternate approach developed in the early days of the project. Diodes, rather than a latching relay, were used to isolate the redundant preamplifier sections and switch from one to the other. This approach had the advantage of very high reliability, since no electromechanical component was required in the preamplifier. However, the use of diodes limited the output amplitude of the preamplifier, and they were abandoned in favor of the relay switch described in the body of this report.

Figure C1 shows, in greatly simplified form, the redundant preamplifier, cable, and termination circuit. Power supply voltage E_s is made either positive or negative with respect to ground. If E_s is positive, the top amplifier $A1$ is energized while $A2$ is shut off. If E_s is made negative, the situation is reversed: $A2$ is energized while $A1$ is shut off. Diodes $CR3$ and $CR4$ isolate the preamplifiers from each other, since one diode is always back biased.

Figure C2 shows the circuit with positive E_s. In this case, dc current flow is out of E_s, through the cable center conductor, through $CR3$ and $R1$ to the top preamplifier. Zener diode $CR1$ establishes a supply voltage of +15 V dc across $A1$. Notice that $CR4$ is back biased, which makes it appear as an open circuit, thus isolating the bottom preamplifier. The audio signal from the hydrophone is coupled into $A1$, where it is amplified. The output of $A1$ is coupled to the load via $C3$ and $C5$. As long as $CR3$ remains forward biased, the audio signal passes right through this diode unaltered.

Figure C3 shows the circuit with negative E_s. In this case, dc current flow is out of ground through the cable shield to the bottom preamplifier, returning through the cable center conductor

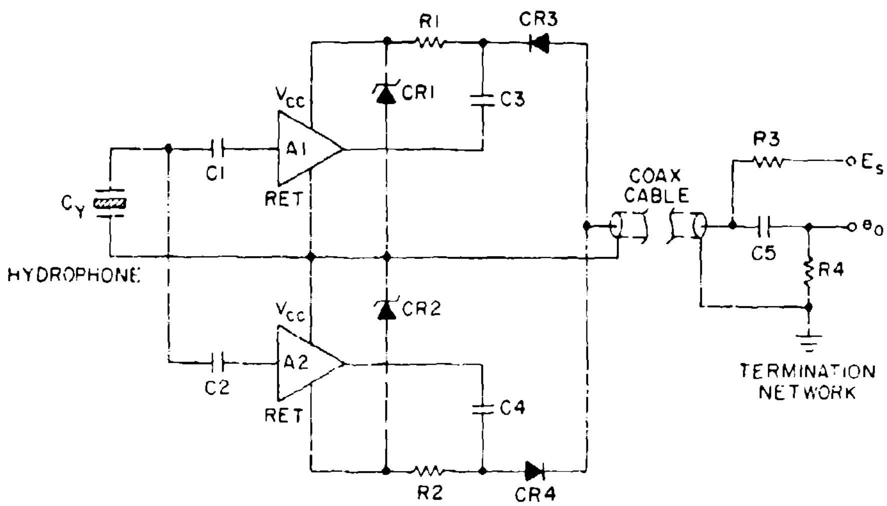

Fig. C1 Simplified schematic of redundant preamplifier with diode switch

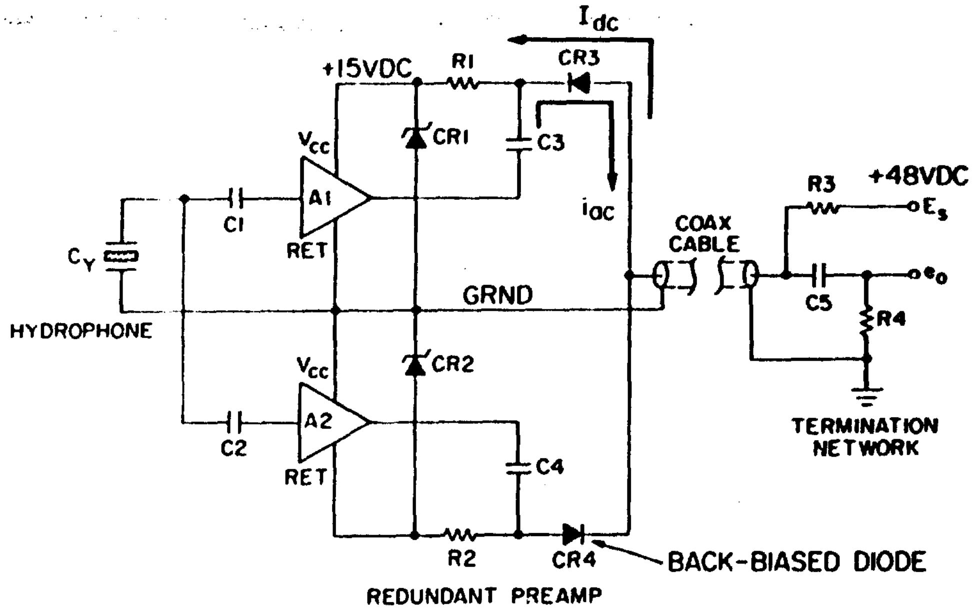

Fig. C2 — Circuit conditions for positive E_s

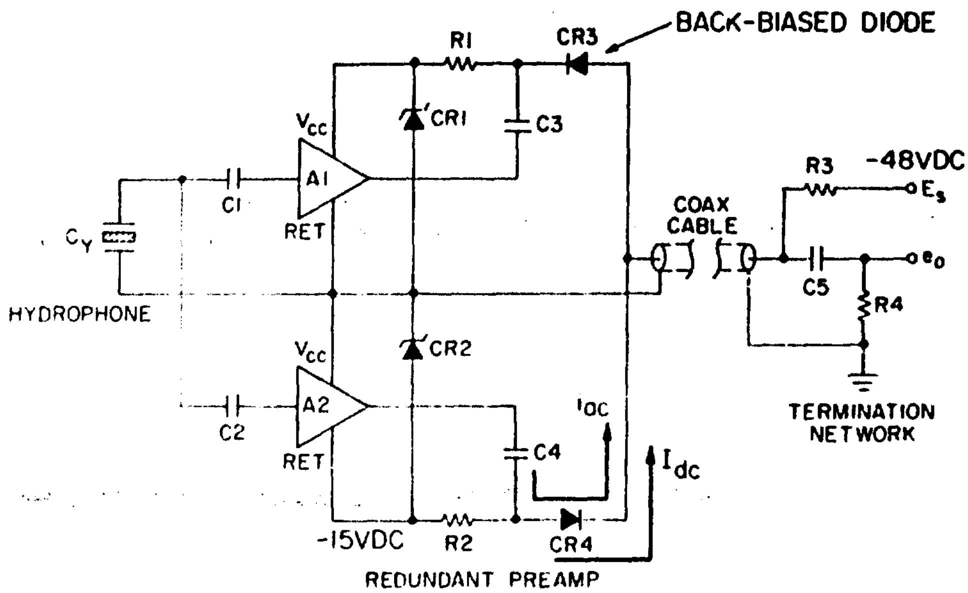

Fig. C3 — Circuit conditions for negative E_s

to E_s. Zener diode $CR2$ establishes +15 V dc across $A2$. Diode $CR3$ is back biased, isolating the top preamplifier. Audio is coupled through $C4$ and $C5$ to the load.

While redundancy makes this circuit practically fail-safe, it also exacts a penalty. From Fig. C2, we notice that the audio signal will pass through $CR3$ unaltered only as long as $CR3$ remains forward biased. The instantandous current in $CR3$ must always be positive if $CR3$ is to remain forward biased. Hence, one can get back as load current only what one delivers as supply current.

This is clarified by Fig. C4, in which we see that the peak ac load current obtainable is equal to the dc supply current. Beyond this point, the output is clipped because *CR*3 does not allow reverse current flow. A few numbers might be helpful. Assume that the 50-Ω coaxial cable is term[illegible]ated in a 50-Ω impedance. To develop 1 V rms across this load requires a peak output current of 1.414/50 or 28.3 ma. The dc supply current must be at least this great to avoid output clipping. Hi[illegible]er output levels would require higher supply currents. A similar analysis could be made for the co[illegible]ditions of Fig. C3. The limitation would vanish if the diodes were removed, but *CR*3 and *CR*4 are necessary for circuit redundancy.

Figure C5 shows a practical implementation of this approach for the H68B hydrophone.

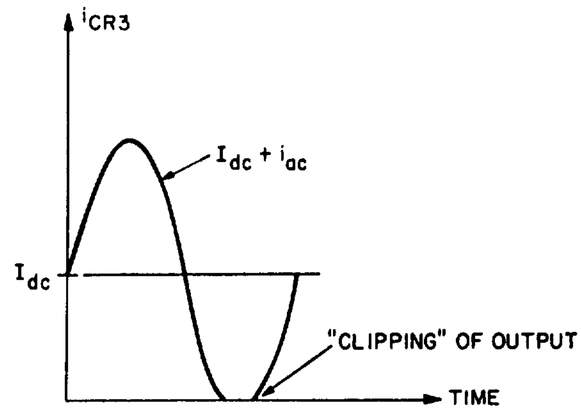

Fig. C4 — Instantaneous current in *CR*3 for circuit of Fig. C2, showing output clipping

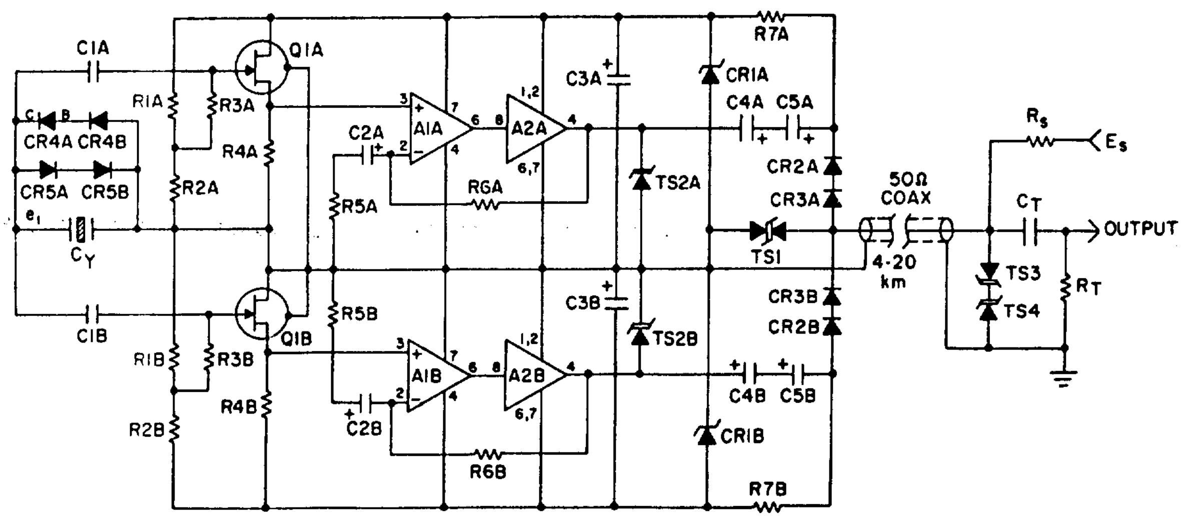

Fig. C5 — Redundant preamplifier with diode switch

Appendix D

PREAMPLIFIER PROOF TESTS

The following tests and measurements were required by the program sponsor to certify the H68B preamplifier design for acceptance.

Environmental tests consisted of burning in the preamplifier at 125°C for 160 h, during which time one preamplifier section was continuously powered at nominal current +10%. The other preamplifier section was not energized.

The following measurements were conducted both before and after the environmental tests:

(1) Determining and recording the gain of each preamplifier section as a function of frequency for frequencies between 0.1 and 100 kHz for input levels of -83, -63, and -43 dBV.

(2) Determining and recording the equivalent noise input level of each preamplifier section as a function of frequency for frequencies between 0.1 and 100 kHz. The transducer input to the preamplifier was simulated by a 140-pF disc ceramic capacitor.

(3) Determining and recording the maximum output signal level at 1% total harmonic distortion (output clipping) for each preamplifier section at frequencies of 10, 13, 20, and 40 kHz for

(a) nominal power supply current,

(b) nominal current +10%, and

(c) nominal current -10%.

For all functional tests the preamplifier load was a 50-Ω coaxial cable terminated in an HTS or other circuit having identical termination impedance.

No degradation of the preamplifier operating characteristics resulted from the environmental tests.